PNAS

Supporting Information for

Targeting MYC induces lipid droplet accumulation by upregulation of HILPDA in clear cell renal cell carcinoma

Lourdes Sainero-Alcolado[1], Elisa Garde-Lapido[1], Marteinn Thor Snaebjörnsson[2], Sarah Schoch[3], Irene Stevens[4], María Victoria Ruiz-Pérez[1], Christine Dyrager[5], Vicent Pelechano[4], Håkan Axelson[3], Almut Schulze[2], and Marie Arsenian-Henriksson[1,*]

[1]Department of Microbiology, Tumor and Cell Biology (MTC), Biomedicum B7, Karolinska Institutet, 17165, Stockholm, Sweden.
[2]Division of Tumor Metabolism and Microenvironment, German Cancer Research Center (DKFZ), 69120, Heidelberg, Germany.
[3]Division of Translational Cancer Research, Department of Laboratory Medicine, Lund University, 221 00, Lund, Sweden.
[4]Science for Life Laboratory, Department of Microbiology, Tumor and Cell Biology (MTC), Karolinska Institutet, SE-171 65, Stockholm, Sweden.
[5]Department of Chemistry-BMC, Uppsala University, 75123 Uppsala, Sweden.

*Corresponding author: Marie Arsenian-Henriksson, marie.arsenian.henriksson@ki.se

This PDF file includes:

Supporting Materials and Methods

Cell lines and cell culture

Three different clear cell renal cell carcinoma cell lines RCC4 (male), 786-O (male), and A498 (female) with loss of *VHL* (RCC4 *VHL*-, 786-O *VHL*-, and A498 *VHL*-) or with *VHL* reintroduced (RCC4 *VHL*+, 786-O *VHL*+, and A498 *VHL*+) were used. The RCC4 cells were maintained in high glucose DMEM with 10% FBS and 1% geneticin (Gibco, Life Technologies). The 786-O and A498 cells were cultured in high glucose DMEM (Gibco, Life Technologies) with 10% FBS (Cytiva, EU approved, heat inactivated) and 1% penicillin/streptomycin (Gibco, Life Technologies). All cells were cultured in a humidified environment at +37°C and 5% CO_2. The identity of all ccRCC cell lines was verified by STR analyses (European Collection of Authenticated Cell Cultures, ECACC). The RCC4 *VHL*+ and *VHL*- cell lines were purchased from The European Collection of Authenticated Cell Cultures (ECACC), with catalogue number 03112702 and 03112703. The 786-O and A498 *VHL*+ and *VHL*- cell lines were generously shared by Assoc. Prof. Susanne Schlisio (Karolinska Institutet), where the *VHL*+ cells were generated by transfection of the *VHL*- cells with the pRc/CMV-HA-VHL (WT7) vector as previously described (1). The tumor cell lines used in the LD screening, were either purchased from ATCC or generously shared by other Swedish research Labs.

The original RCC4 *VHL*+ and *VHL*- cells were transiently transduced with lentiviruses carrying one short hairpin RNA against MYC, pLKO.1 puro non-mammalian sh*MYC* (TRCN0000039640) (Merck/Sigma-Aldrich), (RCC4 *VHL*+ sh*MYC* and RCC4 *VHL*- sh*MYC*), and the corresponding empty vector (EV) control (pLKO.1 puro non-mammalian sh*EV*) (RCC4 *VHL*+ sh*EV* and RCC4 *VHL*- sh*EV*). MOI=5 and 4 µg/ml of polybrene (Merck/Sigma-Aldrich) were used for both RCC4 *VHL*+ and RCC4 *VHL*- cells.

786-O *VHL*+ and *VHL*- cells were transduced with lentiviruses carrying the doxycycline inducible pTRIPZ-RFP-EV or pTRIPZ-OMOMYC-RFPshEV vector using MOI=5 and 4 µg/ml polybrene (Merck/Sigma-Aldrich). Stable cell lines were generated by puromycin selection at a concentration of 2 µg/ml for 786-O *VHL*+ and 4 µg/ml for 786-O *VHL*- cells. After 48 h of treatment, cells were maintained in half of the initial puromycin concentration.

For *HILPDA* overexpression, RCC4 and 786-O *VHL*+ and *VHL*- cells were transduced with lentiviruses carrying the pLV[Exp]-Puro-EF1A>hHILPDA[NM_001098786.2], construct or the control pLV[Exp]-EGFP:T2A:Puro-EF1A>mCherry vector, using MOI=5 and 4 µg/ml polybrene (Merck/Sigma-Aldrich). Stable cell lines were generated by puromycin selection at a concentration of 1 µg/ml for RCC4 *VHL*+, 2 µg/ml for RCC4 *VHL*- and 786-O *VHL*+ or 4 µg/ml for 786-O *VHL*- cells. After 48 h of treatment, cells were maintained in half of the initial puromycin concentration.

For generation of 786-O *VHL*- Omomyc cells with *HILPDA* downregulation, we performed transduction with lentiviruses carrying a short hairpin RNA against *HILPDA*, pLV[shRNA]-Puro-U6>hHILPDA[shRNA] establishing 786-O *VHL*- Omomyc sh*HILPDA* cells or with the scramble control pLV[shRNA]-EGFP:T2A:Puro-U6>Scramble_shRNA generating 786-O *VHL*- Omomyc sh*SCR* cells. MOI=5 and 4 µg/ml polybrene (Merck/Sigma-Aldrich) were used for both transductions and stable cell lines were generated by puromycin selection with 4 µg/ml. After 48 h of treatment, cells were maintained in half of the initial puromycin concentration.

Treatment of cells with MYC and metabolic inhibitors

All cells used for the lipid droplet screening were treated with the following concentration of the respective MYC inhibitors (MYCis) 30-60 µM 10058-F4 (F4), 20-40 µM 10074-G5 (G5), or 2-5 µM JQ1. Throughout the study, RCC4, 786-O, and A498 cells were treated with 60 µM F4, 40 µM G5, or 5 µM JQ1. The concentration of other small inhibitors and compounds were 10 µM BPTES, 25 µM L-DON, 5 µM UB006, 10 µM TOFA, 10 µM (RCC4 and A498) or 15 µM (786-O) LD-BTD1, 20

nM chetomin, and 1 µg/ml doxycycline (DOX). DMSO was used as control except for experiments with DOX or L-DON where water was employed. All compounds were purchased from Merck/Sigma-Aldrich, except UB006 which was a generous gift from Dr. Laura Herrero Rodriguez, University of Barcelona, Spain, and LD-BTD1 which was synthesized in the Lab of Associate Professor Christine Dyrager, Uppsala University, Sweden.

Hypoxia chamber experiments

Cells were seeded in plates and were treated the following day with different inhibitors as indicated in each Figure legend. After treatment, cells were cultured in an Invivo$_2$ hypoxia workstation (Baker) during 72 h. Next, cells were fixed or harvested for the different experiments.

Cell viability assay

To evaluate cell proliferation, cells were seeded in 12 well plates and treated during 72 h with MYCis or vehicle. After incubation, cells were trypsinized, mixed with Trypan Blue (Merck/Sigma-Aldrich) and counted in a hemocytometer chamber under an inverted microscope.

BrdU proliferation assay

Cells were seeded in 96 well plates. After 72 h of treatment with the indicated inhibitors or siRNA, proliferation was measured using CyQUANT™ Cell Proliferation Assay kit (Molecular Probes), according to the manufacturer's instructions. After 1 h of incubation, fluorescence was measured using a SpectraMax i3x reader (Molecular Devices) with SoftMax Pro version 7.1 software.

Western blot

Whole-cell extracts were harvested in RIPA lysis buffer (Merck/Sigma-Aldrich) containing protease and phosphate inhibitor cocktail (Thermo Fisher Scientific) after washing with cold PBS. Protein concentration was determined by BCA protein assay (Merck/Sigma-Aldrich) and 20 µg of protein were separated on a 4-12% SDS-PAGE gel (Bolt Bis-Tris Plus, Invitrogen) with Page RulerTM Plus (Thermo Fisher Scientific) molecular weight markers. Proteins were transferred to a nitrocellulose membrane using BioRad Trans-blot turbo (BioRad) followed by staining with Ponceau to verify equal protein transfer. After blocking in 5% non-fat milk (AppliChem GmbH), membranes were incubated at +4°C overnight with the following primary antibodies: mouse anti-c-MYC (Santa Cruz, sc-40) (1:1000), rabbit anti-VHL (Abcam, ab83307) (1:500), rabbit anti-HIF1-α (Novus Biologicals, NB100-479) (1:500), rabbit anti-HIF2-α (Abcam, ab199) (1:1000), mouse anti-Omomyc (Cancer Tools, 21-1-3) (1:1000), or mouse anti-β-actin (Santa Cruz, sc-47778) (1:10,000). Next day, membranes were incubated with goat anti-mouse or goat anti-rabbit secondary antibodies (P044801-2 and P044701-2; Agilent Technologies). Bands were detected using SuperSignalTM West Dura (Cat No.34076; Thermo Fisher Scientific) and imaged in a ChemiDoc XRS+ (Bio Rad). Blots of at least three independent experiments were quantified using ImageJ (NIH) (2).

Oil-red O and LD-BTD1 staining of lipid droplets

Cells grown on glass coverslips were treated during 72 h with MYCis at the indicated concentrations. Following treatment, cells were fixed in cold 4% paraformaldehyde (Merck/Sigma-Aldrich) before incubating with 60% isopropanol (Merck/Sigma-Aldrich) for 5 min. Next, a 3:2 solution of filtered 0.3% Oil-red O solution (Merck/Sigma-Aldrich) and distilled water was added to the coverslips, and after 5 min they were washed three times in water.

For staining of mouse tumors, they were excised, snap-frozen in dry ice and embedded in Optimal Cutting Temperature (OCT) compound (VWR). Tumors were cut in 10 µm sections using a NX70 cryostat (Epredia), and stained with a 3:2 solution of filtered 0.4% Oil-red O and distilled water during 5 min. After incubation, sections were washed for 30 min with distilled water in agitation.

For visualization using LD-BTD1, cells were seeded in six well plates and treated with MYCis in combination with 15 µM (for 786-O cells) or 10 µM (for RCC4 and A498 cells) LD-BTD1 dissolved in DMSO. Cells were then fixed in 4% paraformaldehyde and incubated for 5 min with DAPI (Merck/Sigma-Aldrich; 1:10,000) to stain nuclei. Thereafter, fixed cells were washed three times in PBS.
Tumor sections were stained with LD-BTD1 (1:500 dilution from 10 mM stock) for 5 min, washed three times with PBS and mounted using DAPI-containing mounting media (Bionordika).
All images were captured with a Zeiss Axiovert 200M microscope with the Zen 2 blue edition software. Images were merged using Adobe Photoshop CS6 (Adobe).

RT-qPCR

Total RNA was harvested using TRIzol reagent (Invitrogen) and extracted with DirectZol RNA miniprep kit (Qiagen). For cDNA synthesis, iScript cDNA synthesis kit (Bio-Rad) was used according to manufacturer's instructions. *MYC*, *HILPDA*, and *B2M* mRNA expression were evaluated by real-time (RT)-qPCR using iTaq universal SYBR green supermix (BioRad). The reaction was performed on a StepOnePlus Real Time PCR system with the StepOne software v2.3 (Applied Biosystems) according to the manufacturer's instructions. Samples were run in triplicate and normalized to the mRNA levels of *B-2-microglobulin* (*B2M*), used as internal control. Relative mRNA expression was calculated using the ΔΔCT method. Primer sequences used are listed below.

HILPDA: Forward: *5'-AGCATGTGTTGAACCTCTACCT-3'*
Reverse: *5'-GTGGGCTCTGTGTTGGCTAG-3'*
MYC: Forward: *5'-CATCAGCACAACTACGCAGC-3'*
Reverse: *5'-CGTTGTGTGTTCGCCTCTTG-3'*
B2M: Forward: *5'-TGCTGTCTCCATGTTTGATGTATC-3'*
Reverse: *5'-TCTCTGCTCCCCACCTCTAAGT-3'*

Nutrient deprivation experiments

RCC4 or 786-O cells were seeded in complete medium in 12 well plates. Next day, medium was replaced by medium with 70% delipidized serum (PAN-Biotech GmbH, containing 2/3 less lipids than complete serum) and 30% normal serum i.e., approximately 50% reduction in lipid content, 2.5 mM glucose or 0.8 mM glutamine. MYCi were administered in combination with 15 µM (for 786-O cells) or 10 µM (for RCC4 cells) LD-BTD1 for 72h. Cells were then fixed, and fluorescence images captured as described above.

Immunofluorescence

Cells seeded in glass coverslips were fixed in 4 % paraformaldehyde (PFA) (Histolab) and blocked for 1 h at room temperature with blocking solution (5 % goat serum, 0.25 % Triton X-100, 1 % BSA, all from Sigma-Aldrich) prepared in PBS. Next, primary antibody for HILPDA (SC-376704, Santa Cruz Biotechnology) diluted in blocking solution was incubated overnight at +4°C. After washing with PBS, the slides were incubated for 1 h at room temperature with the secondary antibody (AlexaFluor 568 and 488, Thermo Fisher Scientific). After washing with PBS, DAPI (1:10,000; Life Technologies) was used for nuclear stain. Pictures were taken at 40x with inverted Zeiss Axiovert 200M microscope with the Zen 2 blue edition software.

siRNA knockdown of *HILPDA*

RCC4 *VHL*- cells were plated in six well plates. Next day, the cells were transfected with 50 nM siRNA targeting human HILPDA (4392420, Thermo Fisher Scientific) or with negative control siRNA (AM4615, Thermo Fisher Scientific), using lipofectamine RNAiMAX (Thermo Fisher

Scientific). After 72 h, cells were either fixed for LD visualization or immunofluorescence, collected for RNA extraction, or stained with BrDU for proliferation assay.

Lipidomics

RCC4 *VHL*+ or *VHL*- cells were seeded in 100 mm^2 dishes. The next day, cells were treated with 5 µM JQ1 for 72 h, washed with 0.5 ml cold ammonium acetate (154 mM), snap frozen in liquid nitrogen and scraped off in 0.5 ml ice-cold MeOH/H_2O (80/20 v/v). The suspension was transferred to a glass tube and another 0.5 ml ice-cold MeOH/H_2O (80/20 v/v) were added. The internal standard mix (SPLASH LIPIDOMIX) (Avanti Polar Lipids) was used for normalization 10 µl/sample. After addition of 120 µl 0.2 M HCl, 360 µl chloroform, 400 µl chloroform and 400 µl of water with vigorous mixing between the pipetting steps, samples were centrifuged at 3,000g for 10 min. 700 µl of the lower lipid phase was collected and taken to dryness under a stream of nitrogen gas at +40°C. Lipids were then dissolved in 200 µl isopropanol and subjected to LC-MS analysis.

Lipids were separated on a C8 column (Accucore C8 column, 2.6 µm particle size, 50 x 2.1 mm, Thermo Fisher Scientific) mounted on an Ultimate 3000 HPLC (Thermo Fisher Scientific) and heated to +40°C. The mobile phase buffer A consisted of 0.1% formic acid in CH_3CN/H_2O (10/90, v/v) and buffer B of 0.1% formic acid in CH_3CN/IPOH/H_2O (45/45/10, v/v/v). After injection of 3 µl lipid sample, 20% solvent B were maintained for 2 min, followed by a linear increase to 99.5% B within 5 min, which was maintained for 27 min. After returning to 20% B within 1 min, the column was re-equilibrated at 20% B for 5 min, resulting in a total run time of 40 min The flow rate was maintained at 350 µl/min and the eluent was directed to the ESI source of the QE Plus from 2 to 35 min.

MS analysis was performed on a Q Exactive Plus mass spectrometer (Thermo Fisher Scientific) applying the following settings: Scan settings: Scan range – 200-1600 *m/z* in full MS mode with switching polarities (neg/pos) and data-dependent fragmentation; Resolution – 70,000, AGC target – 1E6; Max. injection time – 50 ms HESI source parameters: Sheat gas – 30; Aux gas – 10; Sweep gas – 3; Spray voltage – 2.5 kV; Capillary temperature – 320°C; S-lens RF level – 55.0; Aux gas heater temperature –55°C. Fragmentation settings: Resolution – 17,500; AGC target – 1E5; Max. injection time – 50 ms. Peaks corresponding to the calculated lipid masses (±5 ppm) were integrated using El-Maven (https://resources.elucidata.io/elmaven) (3).

Stable isotope tracing into fatty acids

RCC4 *VHL*+ and *VHL*- cells were seeded in 100 mm^2 dishes. The next day they were treated with DMSO or JQ1 for 12 h, and medium was changed to labelling medium containing 25 mM $U^{13}C_6$-Glucose and 4 mM $U^{13}C_5$-Glutamine, or 25 mM unlabeled glucose and 4 mM $U^{13}C_5$-Glutamine (both from Cambridge Isotopes Laboratories). The cells were then cultured for another 48 h followed by washes with cold 154 mM ammonium acetate, snap frozen in liquid nitrogen and collected in methanol/H_2O (80/20, v/v) with added standards (10 µl of 100 µM Palmitate-2,2-D2 (Eurisotop, DLM-1153-0/ 1x10E^6 cells) 30 µl 0.2 M HCl, 2x 100 µl $CHCl_3$, 2 x 100 µl water was then added with vortexing in between. The suspension was centrifuged at 16,000 g for 5 min, the lower lipid phase was then washed with synthetic polar phase (CH_3 Cl/Methanol/H_2O, 58/33/8, v/v/v) and evaporated to dryness under N_2 at +45°C. For saponification lipids were resuspended in Methanol/H2O (80/20, v/v) containing 0.3 M KOH, heated at +80°C for 1 h and washed twice with 0.5 ml hexane. After addition of 50 µl formic acid, fatty acids were subsequently extracted twice with 0.5 ml hexane and evaporated to dryness under N_2 at +45°C. For LC/MS analysis the lipid phase residue was dissolved in 100 µl isopropanol. For LC/MS analysis of fatty acids 5 µl of each sample was applied to a C8 column (Acclaim RSLC C8 column, 2.2 µm particles, 50 × 2.1 mm, Thermo Fisher Scientific) (at +40°C), with mobile phase buffer A consisting of 0.1% formic acid in CH_3CN/H_2O (10/90, v/v), and solvent B consisting of 0.1% formic acid in CH_3CN/H_2O (90/10, v/v).

The flow rate was maintained at 350 µl/min and eluent was directed to the ESI source of the QE-MS from 3 min to 27 min after sample injection. MS analysis was performed on a Q Exactive Plus mass spectrometer (Thermo Fisher Scientific) applying the following settings: Scan settings: Scan range – 200-1600 *m/z* in full MS mode with switching polarities (neg/pos) and data-dependent fragmentation; Resolution – 70,000, AGC target – 1E6; Max. injection time – 50 ms HESI source parameters: Sheat gas – 30; Aux gas – 10; Sweep gas – 3; Spray voltage – 2.5 kV; Capillary temperature – 320°C; S-lens RF level – 55.0; Aux gas heater temperature –55°C. Fragmentation settings: Resolution – 17,500; AGC target – 1E5; Max. injection time – 50 ms. Peaks corresponding to the calculated fatty acid masses (±5 ppm) were integrated using El-Maven (https://resources.elucidata.io/elmaven) (3) and correction for natural 13C isotopic abundance was performed using IsoCorrectoR (4).

***In vivo* xenograft experiments**

Five-week-old female NMRI-*Foxn1*^{nu} mice (Taconic Biosciences) were housed in pathogen free conditions where light, temperature (+21 °C), and relative humidity (50-60%) were controlled. Food and water were available *ad libitum*. For xenograft experiments, 8 × 10^6 786-O *VHL*- Omomyc or 10 × 10^6 786-O *VHL*- Omomyc sh*SCR* or sh*HILPDA* cells were inoculated subcutaneously into the right flanks of mice. Tumor growth was followed daily, and tumor volume was calculated as width × length × height × 0.52. When tumors reached 0.1 cm^3, they were randomized depending on if they received normal drinking water (-Omomyc) or water containing 1 mg/ml doxycycline (DOX) (Merck/Sigma-Aldrich) and 2% sucrose (Merck/Sigma-Aldrich) (+Omomyc) for tumors from 786-O *VHL*- Omomyc sh*SCR* and sh*HILPDA* cells in four different groups: sh*SCR* -Omomyc, sh*SCR* +Omomyc, sh*HILPDA* -Omomyc, sh*HILPDA* +Omomyc.

For 786-O *VHL*- Omomyc derived tumors, mice were injected intraperitoneally (*i.p.*) with a mixture of 10% DMSO and 90% corn oil (Merck/Sigma-Aldrich) (-BPTES) or 10% BPTES (Merck/Sigma-Aldrich) (12.5 mg/ml/kg) and 90% corn oil (+BPTES), in four different groups: -Omomyc -BPTES (n=6), -Omomyc +BPTES (n=6), +Omomyc -BPTES (n=8), and +Omomyc +BPTES (n=7). Injections were performed daily during the first ten days and then each to every second day. The volume corresponded to 10% of the mouse weight. Animals were monitored every day for signs of weight loss and sacrificed either when the maximum number of 21 injections had been performed or when tumors reached the 1 cm^3 experimental endpoint, both according to the ethical permit. At sacrifice, tumors were dissected and divided in two, one half was fixed in formaldehyde and the other embedded in Optimal Cutting Temperature (OCT) compound (VWR) and snap-frozen in dry ice for further analysis. All procedures were in accordance with the ethical principles and guidelines of Karolinska Institutet and the Swedish law and the ethical permit 19417-2020 approved by the Northern court of Stockholm.

Bulk RNA-sequencing

RNA from cell lysates was isolated using Tri-Reagent and extracted and purified using DirectZol™ RNA MiniPrep kit (Zymo Research), according to the manufacturer's instructions. DNase treatment was used to reduce the amount of genomic DNA. Ribosomal RNA (rRNA) was depleted from the samples using Ribosomal RNA depletion pools (riboPOOLs) developed by siTOOLs Biotech to enable detection of low abundant mRNA and non-coding RNA. RNA was reverse transcribed to cDNA, fragmentation and size selection was performed to purify sequences that were the appropriate length for the sequencing machine. Once the RNA libraries were prepared, they were sequenced using a NextSeq 2000 instrument (Illumina) obtaining 30-40 million reads per sample. Obtained fastq files were mapped to the Ensembl GRCh38 Homo Sapiens reference genome using STAR alignment software version 2.7.8 with Paired End settings (5). Raw abundance measurements were obtained using Subread package version 2.0.3 featureCounts with settings: -

t "exon". Differential gene expression analysis between JQ1 treatment versus DMSO control in both RCC4 *VHL*+ and *VHL*- cell lines was computed using DESeq2 version 1.30.1 (6). Pathway analysis was performed using Reactome (available at http://www.reactome.org) and Metascape (7, 8). Enriched pathways were visualized using Cytoscape Version 3.9.1 and the AutoAnnotate plugin (9). The computations and data handling were enabled by resources in project SNIC2021/22-252 provided by the National Academic Infrastructure for Supercomputing in Sweden (NAISS) at UPPMAX, funded by the Swedish Research Council through grant agreement no. 2022-06725.

Immunohistochemistry on tumor sections

Xenograft tumors were extracted and fixed in 4% paraformaldehyde during 24h and conserved in 70% ethanol at +4°C until they were embedded in paraffin. Tumors were sectioned (10 µm thick) and stained using the EnVision Gl2 Doublestain System (Agilent Technologies) according to the manufacturer's instructions. Paraffin was removed and tumor sections rehydrated using a gradient of xylol-alcohol solutions. Endogenous peroxidase activity was blocked incubating for 30 min in methanol-hydrogen peroxide solution and sections were boiled for antigen retrieval in sodium citrate buffer (pH 6.0). After blocking with a solution containing 1 % bovine serum albumin (BSA), 5 % goat serum, and 0.25% Triton-X in PBS, samples were then incubated overnight at +4°C with primary antibodies; rabbit anti-Ki67 (1:250, ab16667), mouse anti-MYC (1:250, 9402S), rabbit anti-Omomyc (1:500, 21-1-3), or mouse anti-HILPDA (1:250, SC-376704), diluted in blocking solution. Next day, samples were incubated with HRP-polymer (Agilent Technologies) for 20 min, followed by 30 seconds-2 min incubation with 3,3′-Diaminobenzidine (DAB) solution (Agilent Technologies). The Click-iT™ TUNEL Colorimetric IHC Detection Kit (Thermo Fisher Scientific) was used for staining of apoptotic cells following the manufacturer's instructions. For nuclear staining, samples were incubated with hematoxylin (Agilent Technologies), for 2 min, dehydrated by a gradient of alcohol-xylol solutions and mounted with Roti-histokitt mounting medium (Carl Roth). Section images were taken at 40x with inverted Zeiss Axiovert 200M microscope with the Zen 2 blue edition software. The anti c-MYC antibody was purchased from Cell Signaling, anti-HILPDA from Santa Cruz Biotechnologies, anti-KI67 from Abcam, and anti-Omomyc from Cancer Tools.

ENCODE database analysis

The binding peaks for c-MYC and MAX at the promoter of the *HILPDA* gene were analyzed using the University of California Santa Cruz (UCSC) genome browser on human (GRCh37/hg19), and for MIZ-1 the UCSC genome browser on human (GRCh38/hg38), both publicly available in the ENCODE database (10). The upstream and downstream binding base pairs comprising the binding peaks were identified from the DNA sequence obtained from ENCO, later identified by comparing it to the gene sequence using BLAST (https://blast.ncbi.nlm.nih.gov/Blast.cgi).

Analysis of TCGA

TCGA data was downloaded from the GDC data portal (https://portal.gdc.cancer.gov/) using the R package TCGAbiolinks (v.2.24.3) (11). TPM unstranded data of tumor samples was extracted for each tumor type. For comparison of relative gene expression, the data was log2 transformed after adding an offset of 1.

Single-cell RNA-sequencing

Single-cell RNA-seq analysis was performed on data from ccRCC patients obtained from Obradovic *et al* (12). The raw data were downloaded from https://data.mendeley.com/datasets/nc9bc8dn4m/1. The data were separated into adjacent normal tissue and tumor tissue and further filtered to a CD45 negative subset using their previous FACS sorted annotation. These two subsets were separately re-processed in R (v.4.2.1) using Seurat (v.4.1.1) (13) and harmony

(v.0.1.0) (14) was used for data integration. The workflow consisted of an initial QC to remove cells with fewer than 200 and more than 5000 features detected as well as cells with a mitochondrial content of >25%. In addition, only features that were expressed in at least 50 cells were included. Using Seurat's function NormalizeData the data were normalized, and a feature selection was carried out to find the 2000 most variable genes. This was followed by scaling the data using ScaleData and a principal component analysis. For data integration, RunHarmony was used to adjust for patient-to-patient variation. Uniform manifold approximation and projection (UMAP) was performed on the first 20 dimensions of the harmony reductions followed by cluster analysis using the Louvain algorithm implemented in Seurat with a resolution of 0.5. To annotate the clusters, differential gene expression was used by applying Seurat's function FindAllMarkers.

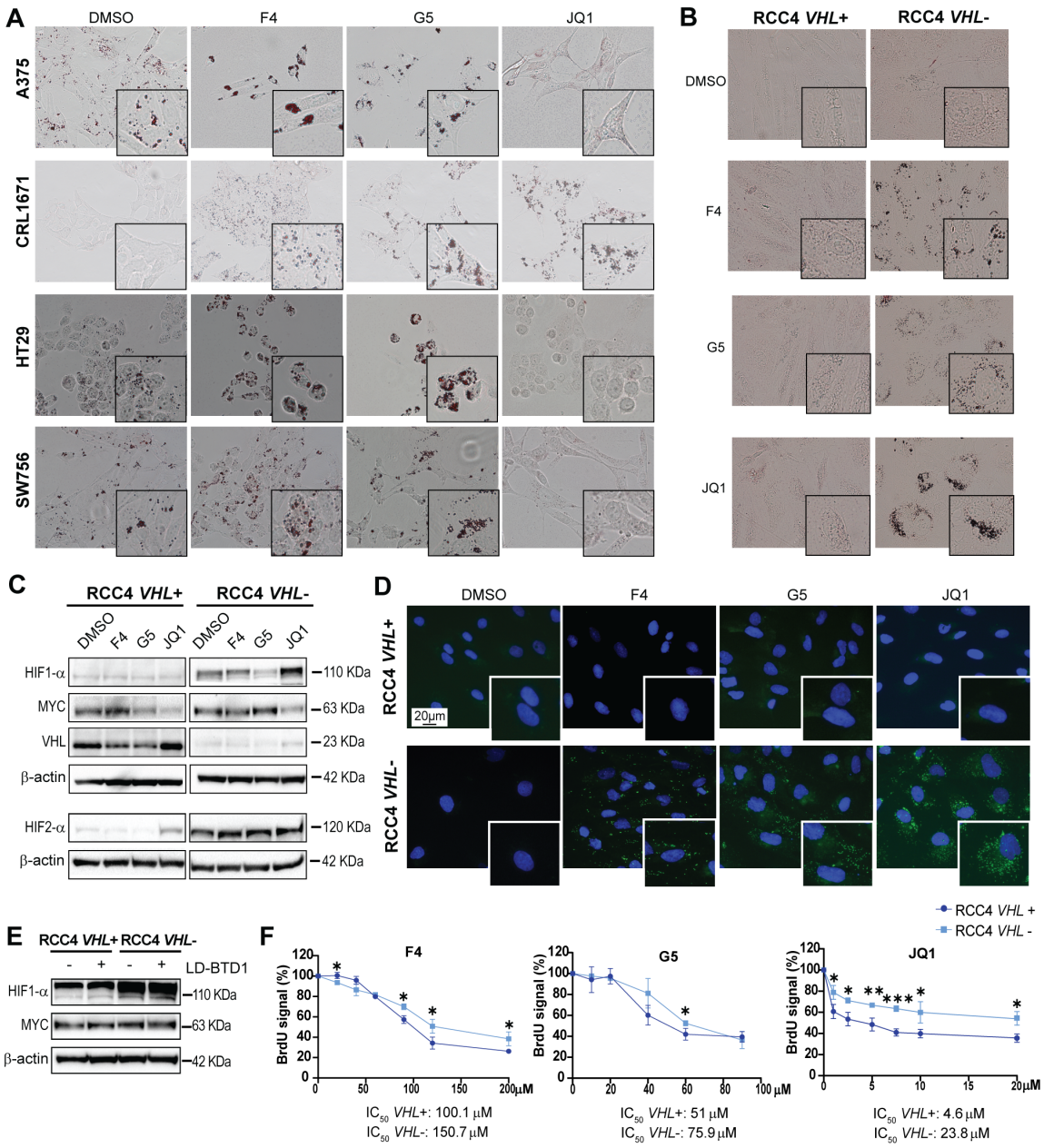

Fig. S1. Related to Fig. 1. HIF stabilization is required for LD accumulation upon MYC inhibition in ccRCC cells. (A and B) Bright field images of lipid droplet stained with Oil-red O (red) (A) in four representative cell lines from the LD screening and (B) in RCC4 *VHL*+ and *VHL*- cells, after treatment with the three MYCis. (C) Western blot of the indicated proteins in RCC4 *VHL*+ and *VHL*- cells after MYCi incubation. (D) Lipid droplet staining in RCC4 *VHL*+ and *VHL*- cells after MYC inhibition. Blue: DAPI; green: LD-BTD1 (staining lipid droplets). Scale bar: 20 μm. (E) Western blot of the indicated proteins in RCC4 *VHL*+ and *VHL*- cells after LD-BTD1 incubation. (F) Graphs representing the proliferation of RCC4 *VHL*+ and *VHL*- cells presented as the percentage of the BrdU signal relative to control after treatment with MYCis. IC_{50} values are shown below the graphs. Data is represented as mean ± SD (n = 3). Statistical analysis: *t*-test, with *, **, and *** indicating p <0.05, <0.01, and <0.001. For all Western blots, β-actin was used as loading control. Molecular

weight markers are shown to the right. All results are representative of three independent experiments.

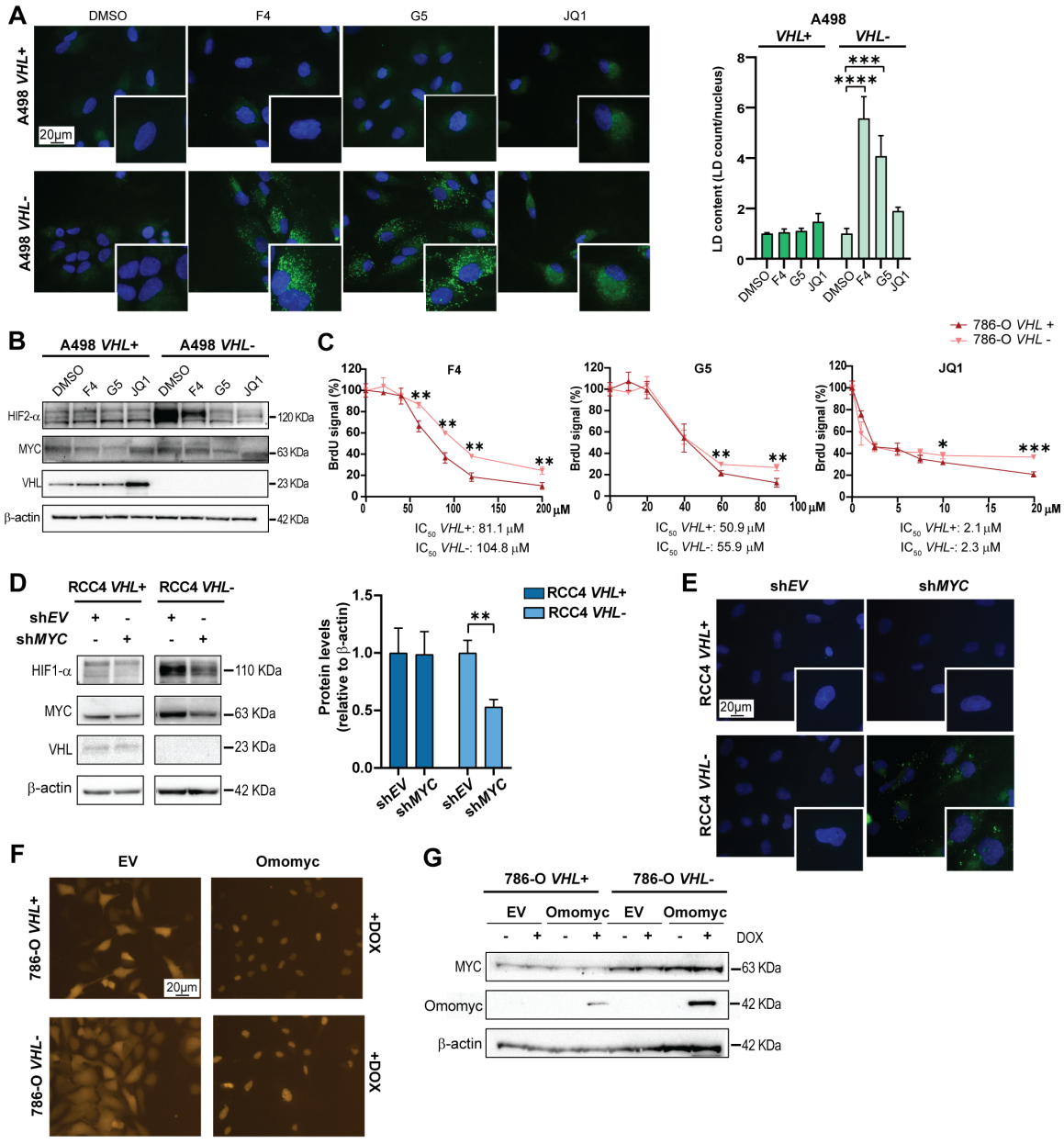

Fig. S2. Related to Fig. 1. HIF stabilization is required for LD accumulation upon MYC inhibition in ccRCC cells. (A) Lipid droplet staining and quantification in A498 *VHL*+ and *VHL*- cells after MYC inhibition. Data is represented as mean ± SD (n = 3). Statistical analysis: one-way ANOVA, with *** and **** indicating p <0.001 and <0.0001, respectively. Blue: DAPI; green: LD-BTD1 (staining lipid droplets). Scale bar: 20 µm. (B) Western blot of the indicated proteins in A498 *VHL*+ and *VHL*- cells after MYCi incubation. (C) Graphs representing the proliferation of 786-O *VHL*+ and *VHL*- cells presented as the percentage of BrdU signal relative to control after 72 h of treatment with MYCis. IC_{50} values are shown below the graphs. Data is represented as mean ± SD (n = 3). Statistical analysis: *t*-test, with *, **, and *** indicating p <0.05, <0.01, and <0.001. (D) Blots of the indicated proteins (left panel) and densiometric analysis of MYC levels (right panel) from RCC4 *VHL*+ and *VHL*- after treatment with a MYC short hairpin (sh*MYC*) or the empty vector (sh*EV*). Data is represented as mean ± SD (n = 3). Statistical analysis: *t*-test, with ** indicating p

<0.01. (E) Lipid droplet staining in RCC4 *VHL*+ and *VHL*- cells after incubation with sh*MYC*, or sh*EV* control. Blue: DAPI; green: LD-BTD1 (staining lipid droplets). Scale bar: 20 μm. (F) Red fluorescent protein (RFP, red) expression in 786-O *VHL*+ EV, 786-O *VHL*+ Omomyc, 786-O *VHL*- EV, and 786-O *VHL*- Omomyc cells after treatment with DOX. Scale bar: 20 μm. (G) Western blot of the indicated proteins in 786-O *VHL*+ EV, 786-O *VHL*+ Omomyc, 786-O *VHL*- EV, or 786-O *VHL*- Omomyc cells after treatment with vehicle (-DOX; DMSO) or DOX. For all Western blots, β-actin was used as loading control. Molecular weight markers are shown to the right. All results are representative of at least three independent replicates.

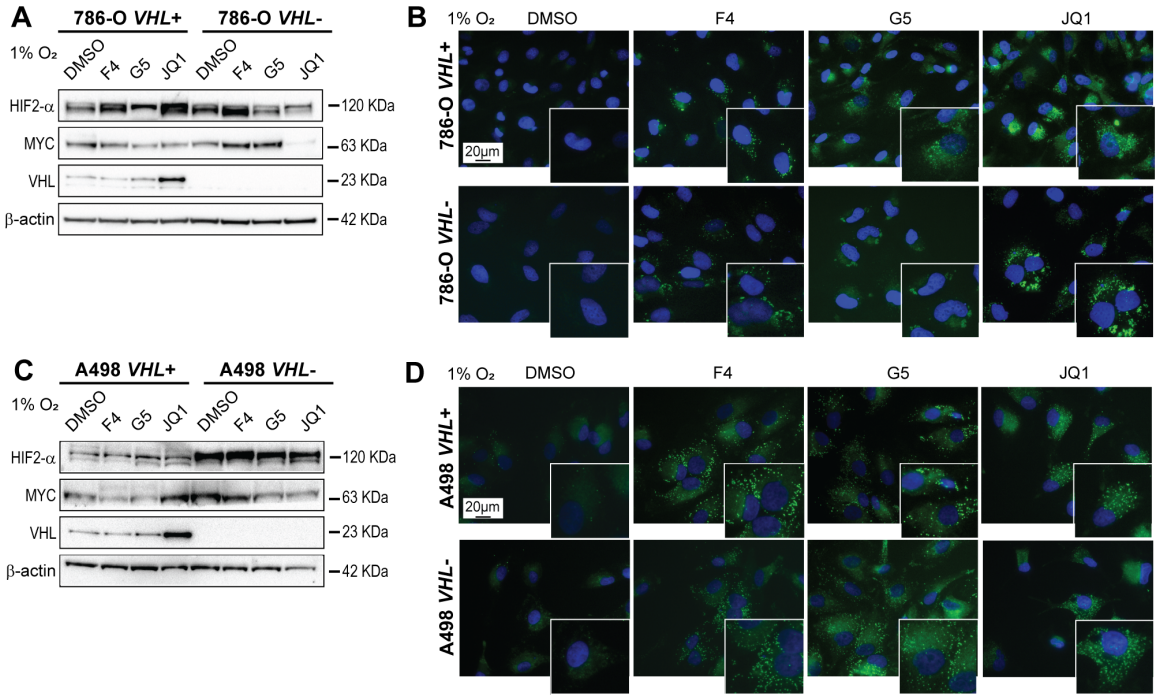

Fig. S3. Related to Fig. 1. HIF stabilization is required for LD accumulation upon MYC inhibition in ccRCC cells. (A) Western blot of the indicated the proteins in 786-O *VHL*+ and *VHL*- cells after treatment with MYCis in 1% O_2 (hypoxia). (B) Lipid droplet staining in 786-O *VHL*+ and *VHL*- cells after treatment with MYCis in 1% O_2 (hypoxia). (C) Western blot of the indicated the proteins in A498 *VHL*+ and *VHL*- cells after treatment with MYCis in 1% O_2 (hypoxia). (D) Lipid droplet staining in A498 *VHL*+ and *VHL*- cells after treatment with MYCis in 1% O_2 (hypoxia). In all fluorescence staining images, blue: DAPI; green: LD-BTD1 (staining lipid droplets). Scale bars: 20 μm. For all Western blots, β-actin was used as loading control. Molecular weight markers are shown to the right. Results are representative of at least three independent replicates.

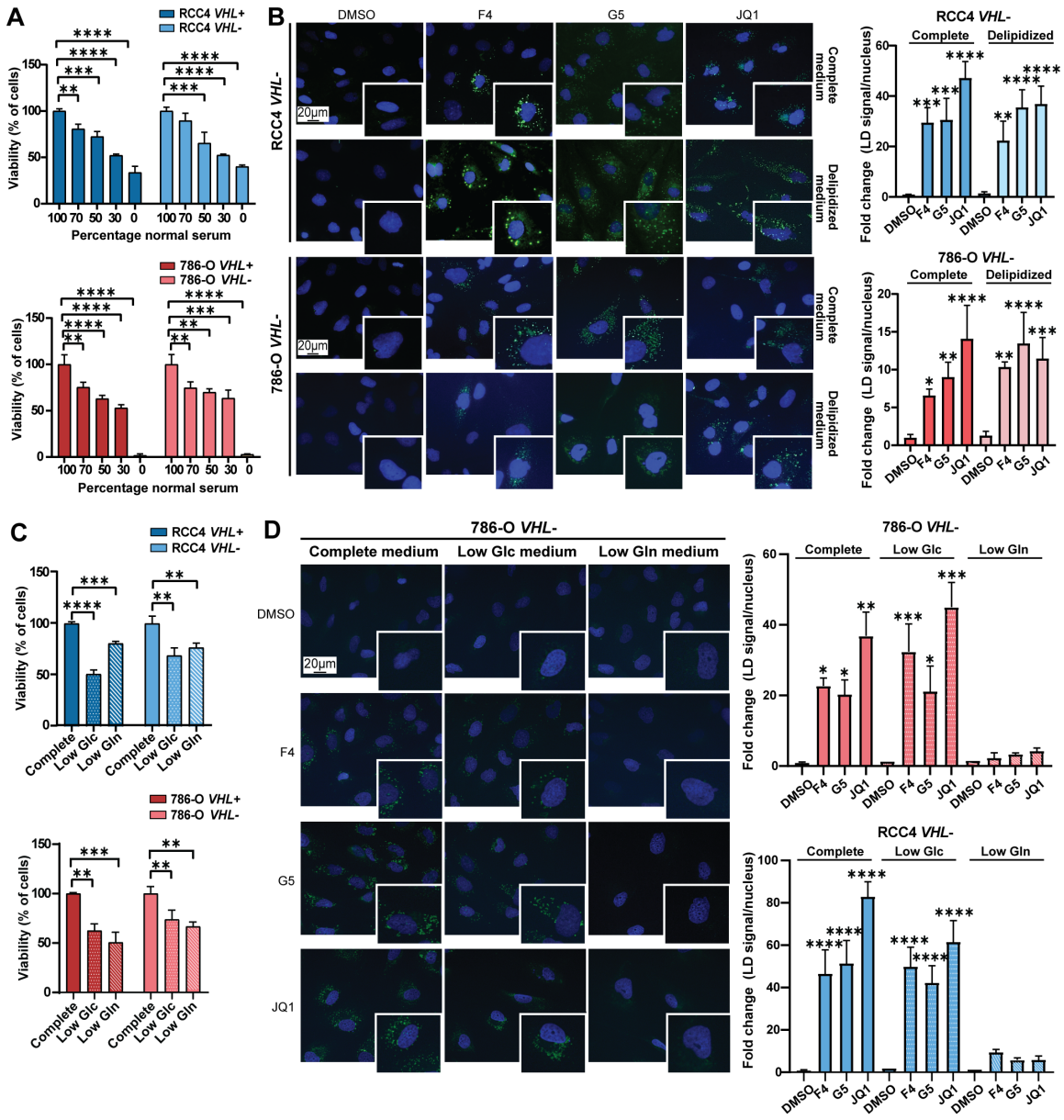

Fig. S4. Related to Fig. 2. Low glutamine levels or inhibition of glutaminase prevent LD formation. (A) Viability graphs represented as percentage of cells compared to control (100% of medium with normal serum) of RCC4 *VHL*+ and *VHL*- cells (upper panel), and 786-O *VHL*+ and *VHL*- (lower panel) quantified by manual cell counting. Cells were cultured in medium with different percentage of normal to delipidized medium (normal to delipidized: 100:0, 70:30, 50:50, 30:70, and 0:100). Data is presented as mean±SD (n = 3). Statistical analysis: One-way ANOVA, with **, ***, and *** indicating p <0.01, <0.001, and <0.001. (B) Lipid droplet staining and quantification in RCC4 *VHL*- and 786-O *VHL*- cells after culture in complete or delipidized medium treated with MYCis as presented. Data is presented as mean±SD (n = 3). Statistical analysis: One-way ANOVA, with *, **, ***, and *** indicating p <0.05, <0.01, <0.001, and <0.001. (C) Viability graphs represented as percentage of cells relative to control (complete medium) of RCC4 *VHL*+ and RCC4 *VHL*- cells (upper panel), and 786-O *VHL*+ and *VHL*- (lower panel) quantified by cell counting. Cells were cultured in complete medium, medium with low glucose (Low Glc), or with low glutamine (Low Gln).

Data is presented as mean±SD (n = 3). Statistical analysis: One-way ANOVA, with **, ***, and *** indicating p <0.01, <0.001, and <0.001. (D) Lipid droplet staining and quantification in 786-O *VHL*- cells and lipid droplet quantification in RCC4 *VHL*- cells shown in Fig. 2A after culture in complete, low glucose (Low Glc) or low glutamine (Low Gln) medium treated with the indicated MYCi. Data is presented as mean±SD (n = 3). Statistical analysis: One-way ANOVA, with *, **, ***, and *** indicating p <0.05, <0.01 and <0.001, and <0.001. In all fluorescence staining images, blue: DAPI; green: LD-BTD1 (staining lipid droplets). Scale bar: 20 μm. Images are representative of three independent replicates.

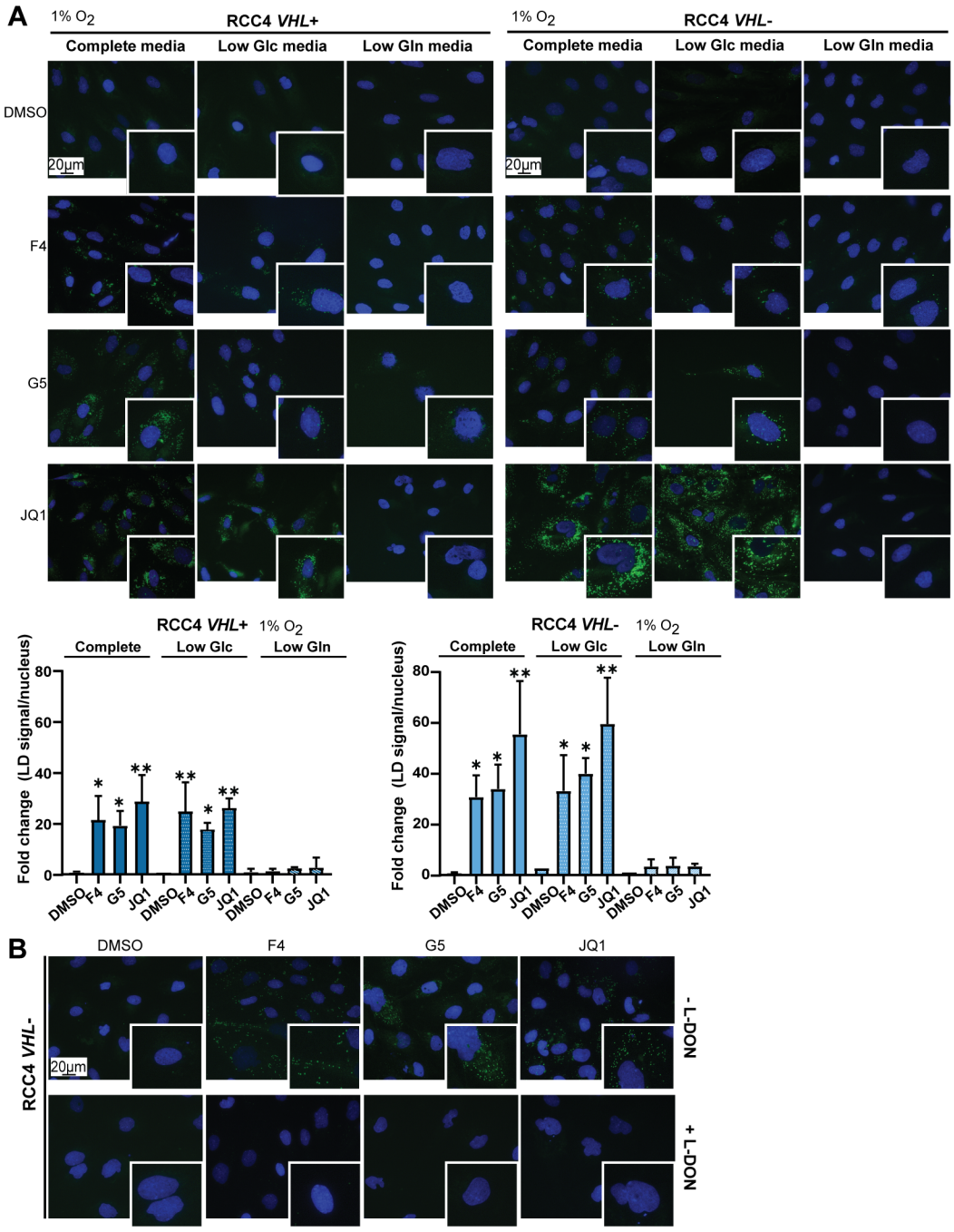

Fig. S5. Related to Fig. 2. Low glutamine levels or inhibition of glutaminase prevent LD formation. (A) Lipid droplet staining and quantification in RCC4 *VHL*+ and *VHL*- cells after culture in complete, low glucose (Low Glc), or low glutamine (Low Gln) medium in 1% O_2 (hypoxia) and treated with MYCis. (B) Lipid droplet staining in RCC4 *VHL*- cells after treatment with DMSO or MYCis alone or in combination with L-DON as indicated. In all fluorescence staining images, blue: DAPI; green: LD-BTD1 (staining lipid droplets). Scale bars: 20 μm. All images are representative of at least three independent replicates.

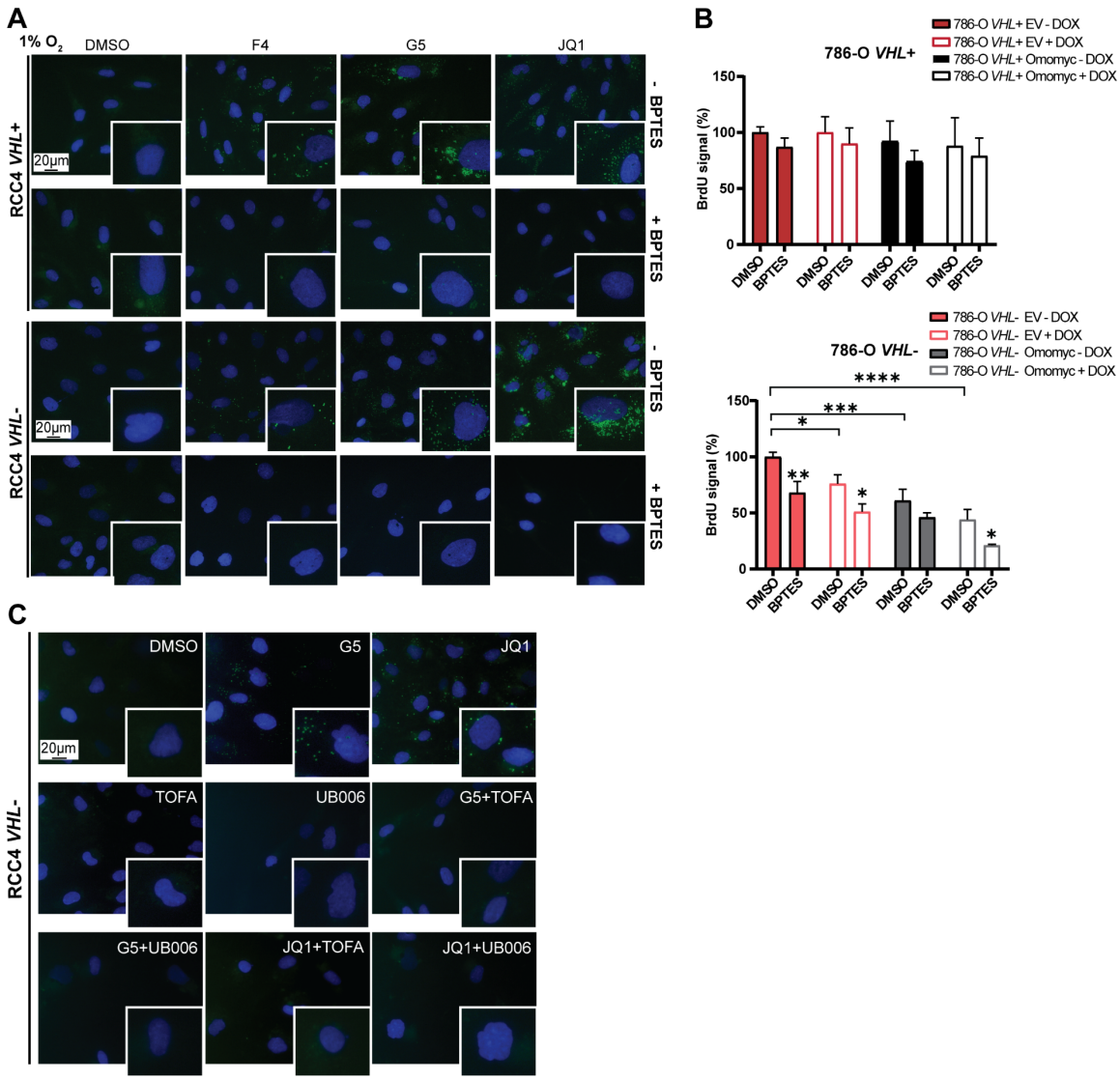

Fig. S6. Related to Fig. 2. Low glutamine levels or inhibition of glutaminase prevent LD formation. (A) Lipid droplet staining in RCC4 *VHL*+ and *VHL*- cells after treatment with DMSO or MYCis alone or in combination with BPTES in 1% O_2 (hypoxia) as indicated. (B) Graphs representing the proliferation of 786-O *VHL*+ (EV and Omomyc) and *VHL*- (EV and Omomyc) cells measured as the percentage of BrdU signal relative to control after treatment with DOX in combination with vehicle (DMSO) or BPTES. Data is represented as mean ± SD (n = 3). Statistical analysis: two-way ANOVA, with *, **, and *** indicating p <0.05, <0.01, and <0.001. (C) Lipid droplet staining in RCC4 *VHL*- cells after treatment with DMSO, MYCis alone or in combination with the fatty acid synthesis inhibitors TOFA or UB006. In all fluorescence staining images, blue: DAPI; green: LD-BTD1 (staining lipid droplets). Scale bars: 20 µm. All images are representative of at least three independent replicates.

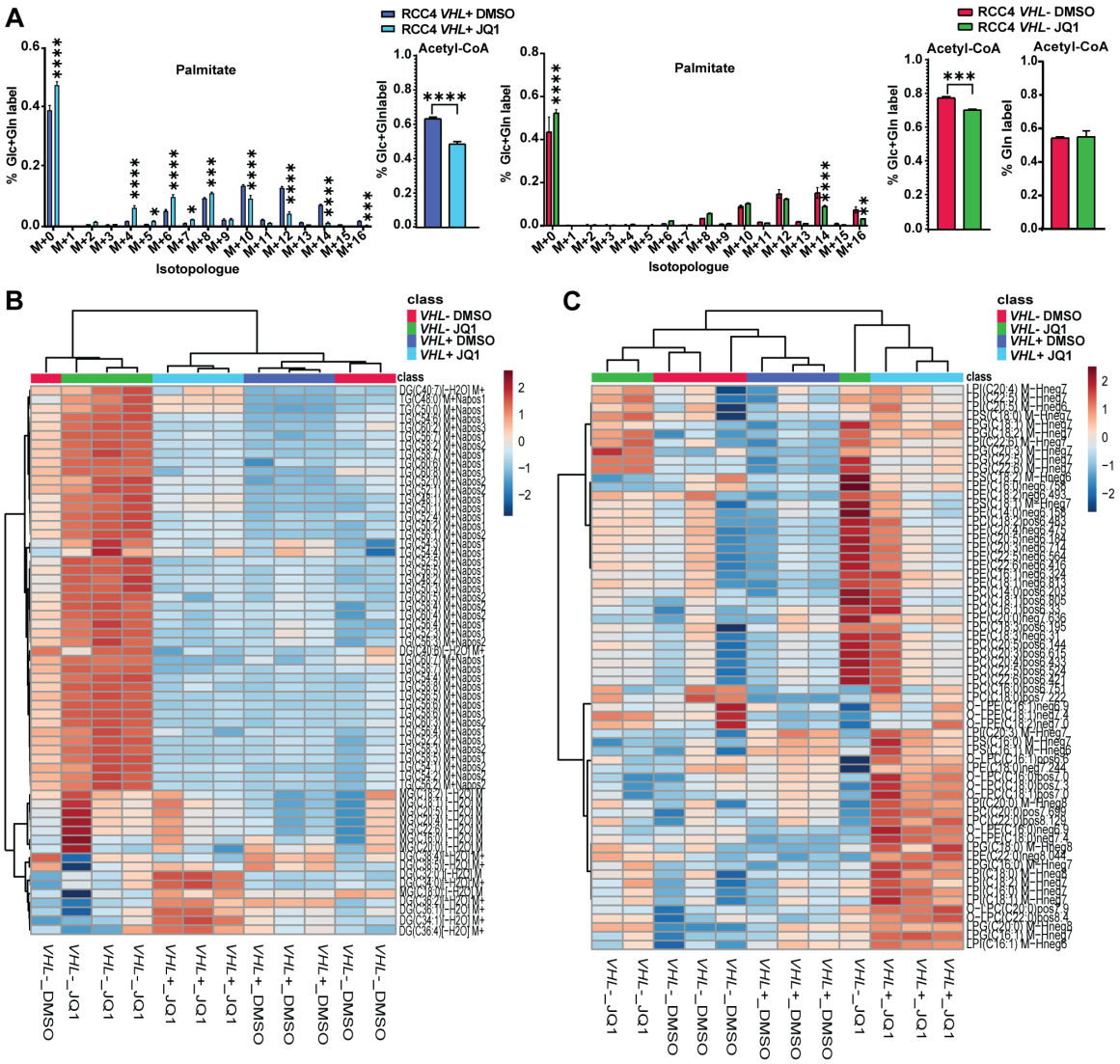

Fig. S7. Related to Fig. 3. Lipidomic analysis reveals different lipid species content in RCC4 *VHL+ versus VHL-* cells. (A) Mass isotopologue distribution of palmitate and cytosolic Acetyl-CoA pool labelling (inferred from the palmitate isotopologue distribution) using U-$^{13}C_6$-glucose and U-$^{13}C_5$-glutamine or U-$^{13}C_5$-glutamine alone in RCC4 *VHL*+ (left panel) and RCC4 *VHL*- cells (right panel) after treatment with JQ1. Data is presented as mean ± SD. Statistical analysis: two-way ANOVA with *, **, ***, and **** indicating p <0.05, <0.01, <0.001, and <0.0001, respectively. (B and C) Heatmaps summarizing the different (B) glycerolipids and (C) lysophospholipids species in RCC4 *VHL*+ and *VHL*- cells after 72 h of treatment with vehicle (DMSO) or JQ1. Color and expression level legends are shown on the top right with red upregulated and blue downregulated lipid species. Lipidomic experiments were performed in three independent replicates.

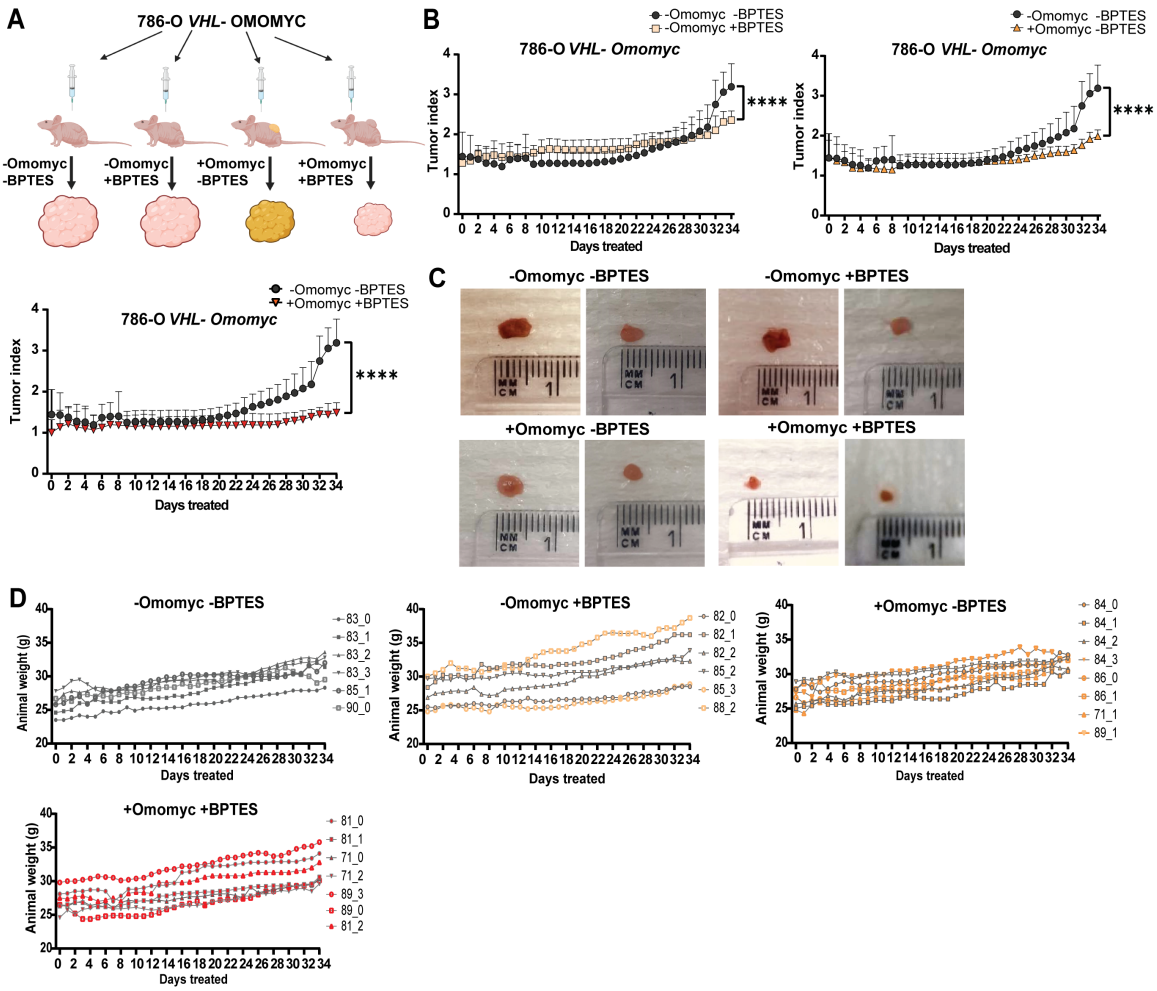

Fig. S8. Related to Fig. 4. Combined inhibition of both MYC signaling and glutamine metabolism results in reduced tumor growth. (A) Illustration representing the treatment scheme for the xenograft experiment using 786-O *VHL*- Omomyc cells. Created with Biorender.com. (B) Tumor index (volume each day/initial volume) in mice with tumors derived from 786-O *VHL*- Omomyc cells treated with -Omomyc -BPTES (n = 6) compared individually to the other groups: -Omomyc +BPTES (n = 6), +Omomyc -BPTES (n = 8), or +Omomyc +BPTES (n = 7). Data is presented as mean ± SD. Statistical analysis: two-way ANOVA with **** indicating $p < 0.0001$, respectively. (C) Representative images of tumors at endpoint. (D) Body weight of all mice from each condition, -Omomyc -BPTES (n = 6), -Omomyc +BPTES (n = 6), +Omomyc -BPTES (n = 8), or +Omomyc +BPTES (n = 7), throughout the xenograft experiment.

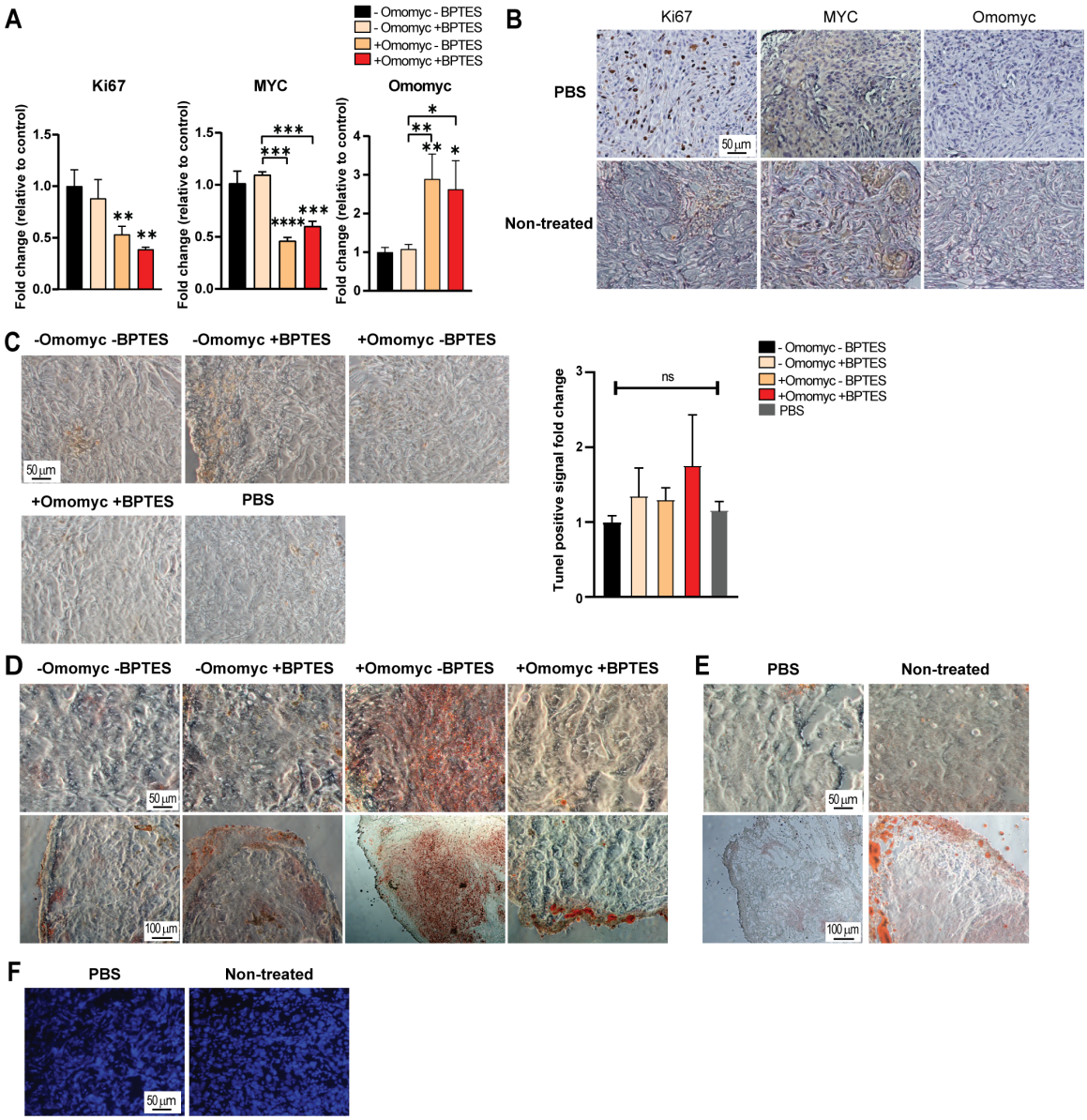

Fig. S9. Related to Fig. 4. Combined inhibition of both MYC signaling and glutamine metabolism results in reduced tumor growth. (A) Quantification of Ki67, MYC and Omomyc from the immunohistochemistry analysis of tumor sections shown in Fig. 4*C*. Data is presented as mean ± SD of at least three different tumors per condition. Statistical analysis: one-way ANOVA with *, **, ***, and **** indicating p <0.05, <0.01, <0.001, and <0.0001, respectively. (B) Immunohistochemistry analysis of tumor sections from PBS- or non-treated mice, stained with anti-Ki67, anti-c-MYC, or anti-Omomyc. (C) Immunohistochemistry analysis and quantification of apoptotic cells using TUNEL assay. Statistical analysis: one-way ANOVA with ns indicating not significant. (D) Tumor sections stained with Oil-red O (red) for LD visualization. Scale bars represent 50 or 100 µm, as indicated. (E and F) Representative images of tumor sections from PBS- or non-treated mice stained with (E) Oil-red O (red) and (F) LD-BTD1 (green) for LD visualization. Blue: DAPI. Scale bars: 50 µm or 100 µm as indicated. All images are representative of at least three different tumors per condition.

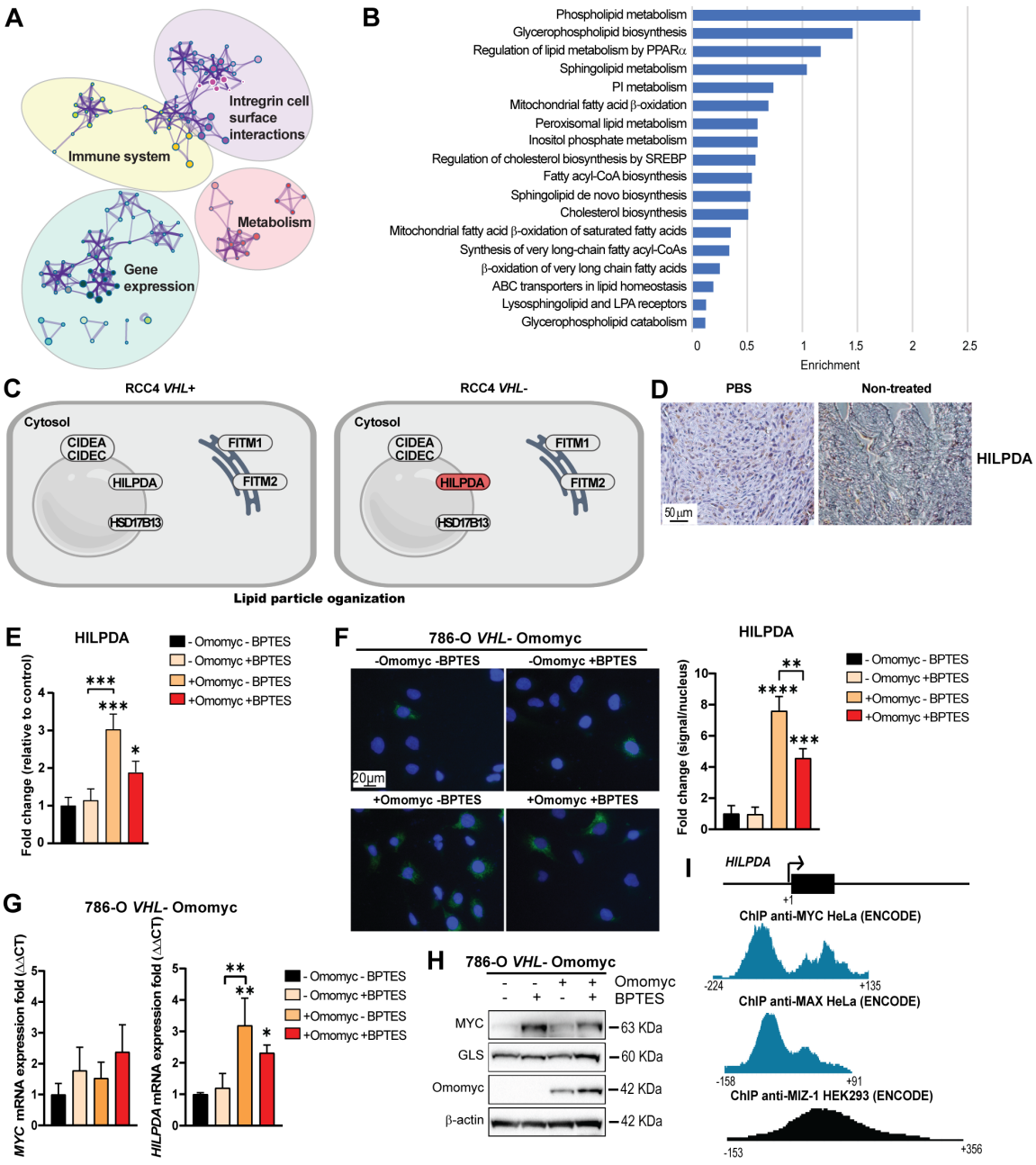

Fig. S10. Related to Figure 5. The LD associated gene *HILPDA* is upregulated in *VHL*- cells after MYC inhibition. (A) Visualization of functional enrichment maps showing biological processes enriched in JQ1-versus DMSO-treated RCC4 *VHL*+ cells (n = 3). The nodes represent significant enriched genes participating in these processes respectively. (B) Bar plot of the most significantly changed lipid metabolic processes in JQ1- *versus* DMSO-treated RCC4 *VHL*+ cells obtained from Reactome analysis. (C) Genes participating in the lipid particle organization related process in RCC4 *VHL*+ cells (left panel) and *VHL*- cells (right panel) after 72 h or treatment with JQ1. In red the significantly upregulated gene *HILPDA*. Image created with Biorender.com. (D) Immunohistochemistry analysis of tumor sections stained with anti-HILPDA in mice administered with PBS or without treatment. Scale bar: 50 µm. (E) Quantification of HILPDA from the immunohistochemistry staining of tumor sections shown in Fig. 5*E*. Data is presented as mean ±

SD of at least three different tumors per condition. Statistical analysis: one-way ANOVA with *, and *** indicating p <0.05 and <0.001, respectively. (F) Immunofluorescence staining and quantification of HILPDA in 786-O *VHL*- Omomyc cells after treatment as indicated. Green: HILPDA; Blue: DAPI. Scale bar: 20 μm. Data is presented as mean ± SD (n = 3). Statistical analysis: one-way ANOVA with **, ***, and **** indicating p <0.01, <0.001, and <0.0001, respectively. (G) RT-qPCR of *MYC* and *HILPDA* in 786-O *VHL*- Omomyc cells after the indicated treatment. *B2M* was used as housekeeping gene. Data is presented as mean ± SD (n = 3). Statistical analysis: one-way ANOVA with * and ** indicating p <0.05 and <0.01. (H) Western blot of MYC, GLS and Omomyc in 786-O *VHL*- Omomyc cells after the indicated treatment. β-actin was used as loading control. Molecular weight markers are shown to the right. (I) MYC, MAX, and MIZ-1 binding peaks at the *HILPDA* promoter in HeLa or HEK293 cells as indicated based on information from the ENCODE database. All results are representative of three independent replicates.

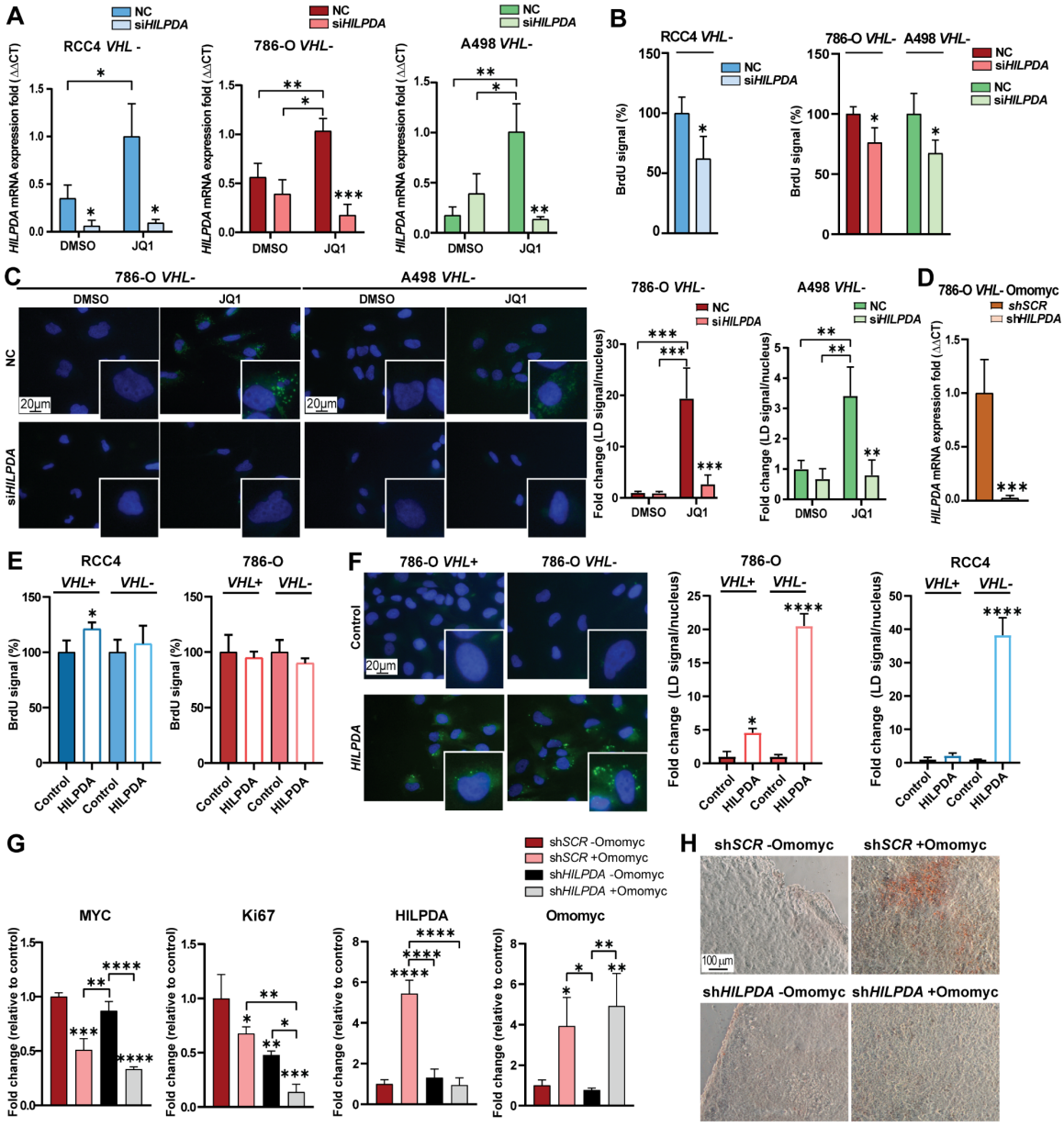

Fig. S11. Related to Fig. 6. Identification of HILPDA as a biomarker for ccRCC. (A) RT-qPCR of *HILPDA* in RCC4, 786-O and A498 *VHL*- cells after incubation with si*HILPDA* or negative control (NC) following treatment with DMSO or JQ1. *B2M* was used as a housekeeping gene. Data is presented as mean ± SD (n = 3). Statistical analysis: *t*-test with *, **, and *** indicating p <0.05, <0.01, and <0.001, respectively. (B) Graph representing the proliferation of RCC4, 786-O, and A498 *VHL*- cells presented as the percentage of the initial BrdU signal relative to control after treatment with si*HILPDA* or negative control (NC). Data is presented as mean ± SD (n = 3). Statistical analysis: *t*-test with * indicating p <0.05. (C) Lipid droplet staining and quantification in 786-O and A498 *VHL*+ and *VHL*- negative control (NC) or si*HILPDA* cells after incubation with DMSO or JQ1. Green: LD-BTD1, blue: DAPI. Scale bars: 20 μm. Data is presented as mean ± SD (n = 3). Statistical analysis: one-way ANOVA with **, and *** indicating p <0.01, and <0.001, respectively. (D) RT-qPCR *HILPDA* in 786-O *VHL*- Omomyc sh*SCR* and sh*HILPDA* cells. *B2M*

was used as a housekeeping gene. Data is presented as mean ± SD (n = 3). Statistical analysis: *t*-test with *** indicating $p < 0.001$. (E) Graph representing the proliferation of RCC4, 786-O *VHL*+ and *VHL*- control and *HILPDA* overexpressing cells presented as the percentage of the initial BrdU signal relative to control. Data is presented as mean ± SD (n = 3). Statistical analysis: *t*-test with * indicating $p < 0.05$. (F) Lipid droplet staining and quantification in 786-O *VHL*+ and *VHL*- control and *HILPDA* overexpressing cells and lipid droplet quantification of RCC4 *VHL*+ and *VHL*- control and *HILPDA* overexpressing cells shown in Fig. 6*B*. Green: LD-BTD1, blue: DAPI. Scale bar: 20 µm. Data is presented as mean ± SD (n = 3). Statistical analysis: *t*-test with * and **** indicating $p < 0.05$ and < 0.0001, respectively. (G) Quantification of MYC, Ki67, HILPDA and Omomyc from the immunohistochemistry analysis of tumor sections shown in Fig. 6*D*. Data is presented as mean ± SD of at least three different tumors per condition. Statistical analysis: one-way ANOVA with *, **, ***, and **** indicating $p < 0.05$, < 0.01, < 0.001, and < 0.0001, respectively. (H) Tumor sections from the indicated treatment groups stained with Oil-red O (red). Scale bar: 100 µm. All results are representative of at least three independent replicates.

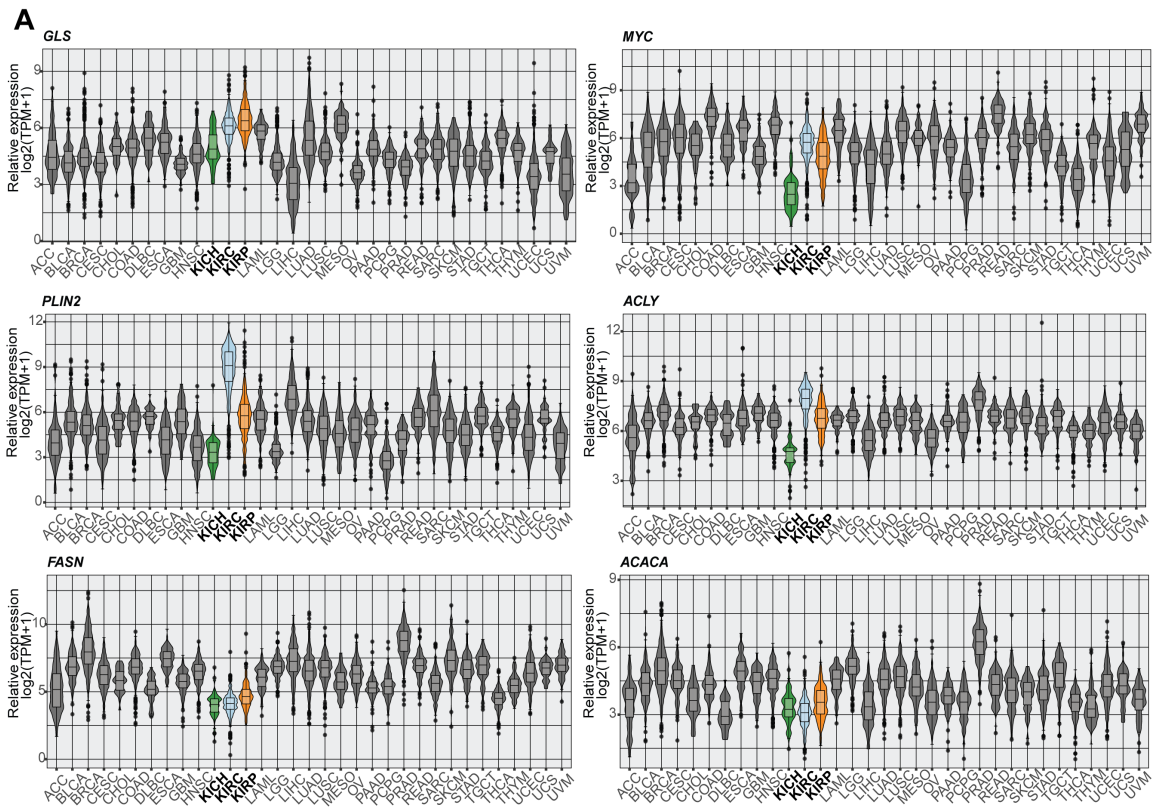

Fig. S12. Related to Fig. 6. Identification of HILPDA as a biomarker for ccRCC. (A) Graphs representing the relative expression of the indicated genes across different cancer types, including the three renal cell carcinomas: clear cell (KIRC) in blue; chromophobe (KICH) in green; and papillary (KIRP) in orange. Analysis was performed on single-cell RNA-sequencing (scRNA-seq) data publicly available from Obradovic *et al* 2021.

Table S1. Summary of the lipid droplet accumulation screening. The screen was performed in different types of human cancer cell lines after treatment during 72 h with three different MYCis as indicated. The type of cancer and the name of each cell line are shown in the first two columns. The presence or absence of lipid droplets in the untreated cells are scored by "Yes" or "No" as presented in the third column. Changes in LD accumulation after incubation with the indicated MYCis compared to untreated cells are presented in the three columns to the right: + indicates increased lipid droplet accumulation, - represents inhibition of LD accumulation, whereas 0 denotes no evident changes in LD accumulation pattern. The ccRCC RCC4 *VHL*- and *VHL*+ cells, respectively are indicated in red and bold.

Tumor type	Cell line	Presence of initial LDs	LD accumulation in response to JQ1	LD accumulation in response to F4	LD accumulation in response to G5
Breast	MCF7	Yes	+	+	+
	MDAMB231	Yes	0	+	+
	T47D	Yes	+	+	0
	SKBR3	Yes	+	+	+
Colon	HCT116	No	0	0	0
	HT29	Yes	-	+	+
	RKO	No	+	+	+
	SW480	Yes	+	+	+
Cervix	SW756	Yes	-	0	+
	HeLa	Yes	+	+	+
	SiHa	No	0	0	+
	ME-180	No	0	0	0
	CaSki	Yes	+	+	+
	C33A	Yes	+	0	+
Endometrial	HTB-112	No	0	0	+
	CRL-1622	No	0	0	0
	CRL-1671	No	+	+	+
Medulloblastoma	DAOY	No	+	0	0
	UW 228-3	No	+	+	+
Prostate	LNCap	No	0	+	0
	DU 145	No	0	+	0
	PNT2	No	0	+	+
	PC -3	Yes	-	+	-
Melanoma	A375	Yes	-	+	+
	MEL 505	Yes	-	+	+
	SKMEL 28	Yes	0	+	+
	BL	Yes	+	+	+
Hepatocarcinoma	HuH7	Yes	0	0	0
	HepG2	Yes	0	0	0
	FLC4	No	0	+	+
Glioblastoma	U87	No	+	0	0
	U251 MC7	Yes	0	0	0
	U3008MG	No	0	0	0
	U3013MG	No	0	0	0
	U3084MG	No	0	0	0
	U3024MG	No	0	0	0
	U3082MG	No	0	0	0
	U3071MG	No	0	0	0
	U3039MG	No	0	0	0
	U3021MG	No	0	0	0
Lung	A549	No	+	+	+
	U1810	Yes	0	+	+
	U1752	Yes	+	+	+
Ovary	NIH:OVCAR3	No	0	+	+

	CAOV-4	No	0	+	+
	CAOV-3	No	0	+	+
Renal	A498	No	+	+	+
	786-O	No	+	+	+
	RCC4 *VHL* -	**No**	**+**	**+**	**+**
	RCC4 *VHL* +	**No**	**0**	**0**	**0**
Osteosarcoma	U2OS	Yes	+	+	+
Neuroblastoma	SK-N-BE(2)	No	+	+	+
	Kelly	Yes	+	+	+
	KCN69n	Yes	+	+	+
	SH-SY5Y	No	+	+	+
	SK-N-SH	Yes	+	+	+
	SHEP	Yes	-	0	0
Supratentorial primitive neuroectodermal tumor	PFSK1	No	+	+	+

Table S2. Abbreviation and name of the different cancer types from TCGA. The abbreviation of the cancer types (left column) and their full name definition (right column).

Abbreviation	Tumor name
ACC	Adrenocortical carcinoma
BLCA	Bladder Urothelial Carcinoma
BRCA	Breast invasive carcinoma
CESC	Cervical squamous cell carcinoma and endocervical adenocarcinoma
CHOL	Cholangiocarcinoma
COAD	Colon adenocarcinoma
DLBC	Lymphoid Neoplasm Diffuse Large B-cell Lymphoma
ESCA	Esophageal carcinoma
GBM	Glioblastoma multiforme
HNSC	Head and Neck squamous cell carcinoma
KICH	Kidney Chromophobe
KIRC	Kidney renal clear cell carcinoma
KIRP	Kidney renal papillary cell carcinoma
LAML	Acute Myeloid Leukemia
LGG	Brain Lower Grade Glioma
LIHC	Liver hepatocellular carcinoma
LUAD	Lung adenocarcinoma
LUSC	Lung squamous cell carcinoma
MESO	Mesothelioma
OV	Ovarian serous cystadenocarcinoma
PAAD	Pancreatic adenocarcinoma
PCPG	Pheochromocytoma and Paraganglioma
PRAD	Prostate adenocarcinoma
READ	Rectum adenocarcinoma
SARC	Sarcoma
SKCM	Skin Cutaneous Melanoma
STAD	Stomach adenocarcinoma
TGCT	Testicular Germ Cell Tumors
THCA	Thyroid carcinoma
THYM	Thymoma
UCEC	Uterine Corpus Endometrial Carcinoma
UCS	Uterine Carcinosarcoma
UVM	Uveal Melanoma

SI References

1. O. Iliopoulos, A. Kibel, S. Gray, W. G. J. Kaelin, Tumour suppression by the human von Hippel-Lindau gene product. *Nat. Med.* **1**, 822–826 (1995).
2. C. A. Schneider, W. S. Rasband, K. W. Eliceiri, NIH Image to ImageJ: 25 years of image analysis. *Nat. Methods* **9**, 671–675 (2012).
3. S. Agrawal, *et al.*, El-MAVEN: A Fast, Robust, and User-Friendly Mass Spectrometry Data Processing Engine for Metabolomics. *Methods Mol. Biol.* **1978**, 301–321 (2019).
4. P. Heinrich, *et al.*, Correcting for natural isotope abundance and tracer impurity in MS-, MS/MS- and high-resolution-multiple-tracer-data from stable isotope labeling experiments with IsoCorrectoR. *Sci. Rep.* **8**, 17910 (2018).
5. A. Dobin, *et al.*, STAR: ultrafast universal RNA-seq aligner. *Bioinformatics* **29**, 15–21 (2013).
6. M. I. Love, W. Huber, S. Anders, Moderated estimation of fold change and dispersion for RNA-seq data with DESeq2. *Genome Biol.* **15**, 550 (2014).
7. M. Gillespie, *et al.*, The reactome pathway knowledgebase 2022. *Nucleic Acids Res.* **50**, D687–D692 (2022).
8. Y. Zhou, *et al.*, Metascape provides a biologist-oriented resource for the analysis of systems-level datasets. *Nat. Commun.* **10**, 1523 (2019).
9. P. Shannon, *et al.*, Cytoscape: a software environment for integrated models of biomolecular interaction networks. *Genome Res.* **13**, 2498–2504 (2003).
10. C. A. Sloan, *et al.*, ENCODE data at the ENCODE portal. *Nucleic Acids Res.* **44**, D726-32 (2016).
11. A. Colaprico, *et al.*, TCGAbiolinks: an R/Bioconductor package for integrative analysis of TCGA data. *Nucleic Acids Res.* **44**, e71–e71 (2016).
12. A. Obradovic, *et al.*, Single-cell protein activity analysis identifies recurrence-associated renal tumor macrophages. *Cell* **184**, 2988–3005.e16 (2021).
13. Y. Hao, *et al.*, Integrated analysis of multimodal single-cell data. *Cell* **184**, 3573–3587.e29 (2021).
14. I. Korsunsky, *et al.*, Fast, sensitive and accurate integration of single-cell data with Harmony. *Nat. Methods* **16**, 1289–1296 (2019).